Novel chemical tyrosine functionalization of adeno-associated virus improves gene transfer efficiency in liver and retina

Aurélien Leray,[a] Pierre-Alban Lalys,[a] Juliette Varin,[b] Mohammed Bouzelha,[b] Audrey Bourdon,[b] Dimitri Alvarez-Dorta,[c] Karine Pavageau,[b] Sébastien Depienne,[a] Maia Marchand,[b] Anthony Mellet,[b] Joanna Demilly,[b] Jean-Baptiste Ducloyer,[b] Tiphaine Girard,[b] Bodvaël Fraysse,[b] Mireille Ledevin,[d] Mickaël Guilbaud,[b] Sébastien G. Gouin,[a] Eduard Ayuso,[b] Oumeya Adjali,[b] Thibaut Larcher,[d] Thérèse Cronin,[b] Caroline Le Guiner,[b] David Deniaud,*[a] and Mathieu Mével*[b]

[a] Dr. A. Leray, P-A. Lalys, S. Depienne, Dr. S.G. Gouin, Pr. D.Deniaud
Nantes Université
CNRS, CEISAM, UMR 6230, F-44000 Nantes, France
E-mail: David.deniaud@univ-nantes.fr

[b] Dr J. Varin, M. Bouzelha, Dr A. Bourdon, K. Pavageau, M. Marchand, A. Mellet, J. Demilly, T. Girard, Dr. B.Fraysse, M. Guilbaud, Dr. E. Ayuso, Dr O. Adjali, Dr T. Cronin, Dr C. Le Guiner, Dr. M. Mével
Nantes Université
TaRGeT, Translational Research for Gene Therapies, CHU Nantes, INSERM, UMR 1089, F-44000 Nantes, France

[c] Dr. D. Alvarez-Dorta
Capacités, 26 Bd Vincent Gâche, 44200 Nantes

[d] Ms M. Ledevin, Dr. T. Larcher
INRAE, Oniris, PanTher, APEX,F-44307 Nantes, France

david.deniaud@univ-nantes.fr, mathieu.mevel@univ-nantes.fr

Abstract: Decades of biological and clinical research have led to important advances in recombinant adeno-associated viruses rAAV-based gene therapy gene therapy. However, several challenges must be overcome to fully exploit the potential of rAAV vectors. Innovative approaches to modify viral genome and capsid elements have been used to overcome issues such as unwanted immune responses and off-targeting. While often successful, genetic modification of capsids can drastically reduce vector yield and often fails to produce vectors with properties that translate across species. Here, we describe a chemical bioconjugation strategy to modify tyrosine residues on AAV capsids using specific ligands, thereby circumventing the need to genetically engineer the capsid sequence. Aromatic electrophilic substitution of the phenol ring of tyrosine residues on AAV capsids improved the *in vivo* transduction efficiency of rAAV2 vectors in both liver and retinal targets. This tyrosine bioconjugation strategy represents an innovative technology for the engineering of rAAV vectors for human gene therapy.

Introduction

Gene therapy with viral vectors has been used in both preclinical and clinical settings to treat cardiovascular[1], muscular[2], metabolic[3], neurological[4], hematological[5] and ophthalmological [6] diseases, as well as infectious disorders [7] and cancers[8]. Owing to their non-pathogenic nature, low immunogenicity, ease of production, and the long-term persistence of transgene expression, recombinant adeno-associated viruses (rAAV) are one of the most widely used viral vector for *in vivo* gene therapy. Several rAAV-based gene therapy products (Luxturna, Zolgensma, Roctavian, Upstaza and Hemgenix)[9–11] have been approved in Europe and the United States. rAAVs thus constitute a promising platform for the treatment of many diseases.

However, while rAAVs are effective as therapeutic gene delivery vehicles, there are several limitations to these vectors that hinder full realization of their potential. First, none of the rAAVs currently used show exclusive tropism for a specific organ or tissue. The high vector doses required to achieve a therapeutic outcome in a given tissue can trigger an immune response that in turn can result in elimination of the transduced cells[12]. Moreover, a large proportion of the population has already been infected with wild-type AAVs and therefore expresses neutralizing anti-AAV antibodies that prevent rAAV-mediated gene transfer. This leads to exclusion of seropositive patients from experimental protocols [13] and limits the use of rAAVs in the general population.

With ever more rAAV-delivered transgenes in clinical trials, there is an unmet need for a new generation of rAAVs with greater transduction efficiency (*i.e*. increased number of transduced cells). A variety of enhancement approaches are described in the literature, most of which involve modification of the viral capsid by genetic engineering (specifically, using rational design or directed evolution approaches)[14]. However, the development of each novel rAAV variant must be accompanied by new bioproduction, manufacturing, purification, and characterization processes.

Site-specific bioconjugation is a burgeoning field of research that enables covalent coupling of ligands (*e.g.* fluorophores, carbohydrates, polymers) to biomolecules. This strategy is largely applied to the development of antibody-drug conjugates[15], and lysine is the most commonly used amino acid for chemical coupling. Lysine residues on the AAV surface have been previously exploited as molecular anchors for the conjugation of amine-reactive molecules. Indeed, our group has previously shown that rAAVs chemically modified with sugars promote cell-

specific transduction and lead to lower levels of serum neutralizing antibodies compared with unmodified rAAVs [16].
Here, we describe a strategy for selective conjugation of ligands on tyrosine (Y) residues present on the surface of the rAAV capsid. The literature describes a wide range of biorthogonal click strategies that allow functionalization of the phenol side chain of Y [17]. Y-targeting is an effective means of designing a wide range of important biomolecules, including antibody-drug conjugates[18], glycovaccines[19], and PEG-conjugates[20]. Because Y residues are neutral over a wide pH range, chemical modification does not alter the overall protein charge. Several studies have described the impact of genetic replacement of a Y with a phenylalanine in the rAAV capsid sequence: this change significantly increases transduction and, in some cases, has been associated with reduced biodistribution and an absence of inflammation in transduced tissues[21–23]. These effects are due to the non-phosphorylated nature of the surface Y: this prevents ubiquitination of the rAAV capsid and consequent degradation by the proteasome. Indeed, Y phosphorylation–dephosphorylation is one of the main post-translational modifications that decreases transduction efficiency[24]. Furthermore, the bioconjugation step is performed on purified rAAVs, meaning that the pre-established bioprocess does not need to be altered. This strategy paves the way for the development of a new method of AAV bioconjugation.

Results and Discussion

Among the different Y bioconjugation reactions, we specifically focused on the diazo-coupling reaction. In this reaction, aryldiazonium salts, prepared from the corresponding aniline by the action of a nitrite in an acidic medium, establish an azo linkage with the phenol side ring of Y *via* electrophilic aromatic substitution[25]. We used two targeting ligands with a reactive diazonium salt coupling function to chemically modify the rAAV2 capsid (Figure 1). The first carries a *N*-acetylgalactosamine (GalNAc) (Figure 1A), a sugar that serves as an asialoglycoprotein receptor (ASGPr) targeting unit for specific liver delivery[26]; and the second a mannose sugar (Man) (Figure 1B). Indeed, this second sugar has been previously used for retinal applications after lysine bioconjugation on rAAV2, with promising results[27].

Before beginning our experiments, we estimated the number of Y residues present on the capsid surface, and therefore the number of reactive functions available for chemical modification. Using AAV2 crystallographic data and the PyMOL Molecular Graphics System, we found a total of 360 potentially accessible Y residues available for covalent coupling on the AAV2 capsid. Next, to target the liver, we designed two GalNAc ligands (Figure 1A): compound **1,** which has a spacer at the anomeric position carrying the reactive diazonium function to perform the coupling; and compound **2**, which lacks a coupling function and is designed to validate the formation of a covalent bond and rule out the possibility of the physical adsorption of the molecule on the AAV2 surface. Diazonium salt **1** was synthesized in 4 steps (Scheme S1) from a protected GalNAc ammonium salt which reacted, in basic medium, with 4-nitrobenzoyl chloride. The hydroxyl groups of GalNAc were deprotected with the basic resin IRN78, and the nitro function was reduced to yield the corresponding aniline. Finally, 1.2 equivalents of tetrafluoroboric acid were added at room temperature, followed by 1.1 equivalents of *tert*-butylnitrite, which, after 5 min of stirring, yielded diazonium **1** in quantitative yield. This final product was used directly for the AAV bioconjugation step. Control compound **2** was prepared in two steps (Scheme S8) from the corresponding ammonium salt through the action of DMAP and benzoyl chloride followed by reaction on IRN78 basic resin to cleave the acetyl groups.
To target the retina, we used a mannose-derived ligand to generate AAV2-Man(Y). Two mannose ligands (Figure 1B) were synthesized using the same protocol described for the GalNAc ligands (Figures S13 and S20). Compound **3** carried the reactive diazonium function to perform the coupling and control compound **4** lacked a coupling function (Figure 1B).
All chemical compounds were characterized by NMR, HPLC, and mass spectroscopy (Figures S2-S24).

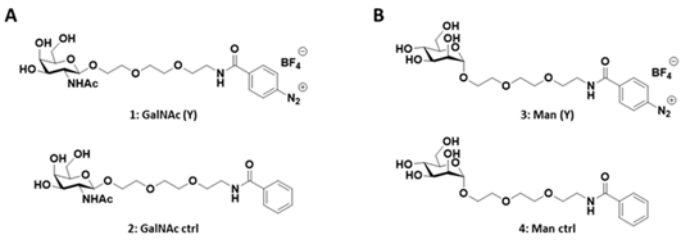

Figure 1: Structure of the GalNAc(Y) and Man(Y) ligands used for bioconjugation on the AAV2 capsid.

Bioconjugation of compounds **1** and **3** on the AAV capsid surface was performed in the conditions described in Figure 2A. Aromatic electrophilic substitution of the phenol of Y was performed at room temperature for 4 h in TBS buffer at pH 9.3. Compounds **2** and **4** were used as negative controls. After titration of the samples, dot blot analysis with A20 antibody, which detects the assembled capsid, indicated that the coupling conditions were not deleterious to the AAV capsid (Figure 2B-C). Moreover, using soybean lectin, which recognizes the GalNAc motif, and concanavalin A, which recognizes the mannose motif, positive dots were observed only for GalNAc(Y) (**1**) and Man(Y) (**3**), which unambiguously confirmed the formation of a covalent diazo linkage between the Y phenol and the diazonium salt (Figure 2B-C).
We also confirmed these results by western blot using a polyclonal antibody and silver staining, which revealed that the three VP capsid subunits remained intact (VP3 = 61, VP2 = 73

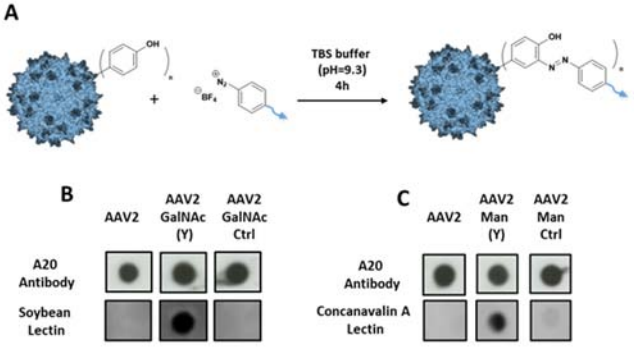

Figure 2: A) Chemical reaction between AAV2 and diazonium salt ligand. B) Dot blot analyses with A20 antibody (assembled capsid detection, top) and soybean lectin (GalNAc detection, bottom). C) Dot blot analyses with A20 antibody (assembled capsid detection, top) and concanavalin A lectin (mannose detection, bottom).

and VP1=87 kDa). It is worth noting the appearance of high molecular weight bands with low intensity after grafting of the GalNAc(Y) and Man(Y) ligands onto the capsid (Figures S25A-C and S26A-C). Western blot analysis using soybean lectin and concanavalin A indicated that covalent coupling on all three AAV capsid proteins (VP1, VP2 and VP3) occurred only with the GalNAc(Y) and Man(Y) ligands. This confirms that the aryldiazonium function was essential for Y bioconjugation (Figures S25B and S26B).
Dynamic light scattering (DLS) also revealed the absence of particle aggregation after coupling. Indeed, the size of AAV2, AAV2-GalNAc(Y) and AAV2-Man(Y) remained around 26 nm.

For *in vitro* evaluation of the biological efficiency of the AAV2-GalNAc(Y), which carries the eGFP transgene under the control of a CAG promoter, two different cell lines were transduced. Because GalNAc sugar allows targeting of the asialoglycoprotein receptor (ASGP-R), which is highly expressed on hepatocytes, murine primary hepatocytes were used as ASGP-R positive cells and HEK293 cells as negative controls[28]. In HEK293 cells, transduction was approximately two times more efficient for AAV2 (90% of GFP+ cells) versus AAV2-GalNAc(Y) (50% of GFP+ cells) at the same multiplicity of infection (MOI; 1E4 for both vectors) (Figure S27). This can be explained by decreased recognition of AAV2 by heparan sulfate proteoglycans after modification of its capsid surface.[29] Y bioconjugation therefore may have detargeted this vector from its natural receptor. On the other hand, in the same experiment using murine primary hepatocytes the transduction efficiency of rAAV2-GalNAc(Y) was 3-fold higher than that observed for the unmodified rAAV2 (Figure S27). These promising results unambiguously demonstrated the efficacy of the bioconjugation of GalNAc sugar on AAV2 for *in vitro* targeting of hepatocytes.
We next examined the transduction efficiency of AAV2-GalNAc(Y) *in vivo*. To study liver transduction, healthy adult mice received an intravenous injection in the tail vein of unmodified rAAV2 or rAAV2-GalNAc(Y) (5E12 vg/kg), both carrying the same CAG-eGFP expression cassette, while a control group was injected with buffer (n=6 per group).
Liver samples were collected at euthanasia 1 month after vector administration for quantification of vector genome copy number by qPCR, eGFP protein expression by western blot, and the percentage of transduced cells by immunohistochemistry. Mean vector genome copy number was significantly lower in mice injected with rAAV2-GalNAc(Y) *versus* unmodified rAAV2 (0.02 vg/dg and 0.64 vg/dg, respectively; p=0.026) (Figure S28). However, in the same liver samples, GFP protein expression was 2-fold higher in mice injected with rAAV2-GalNAc(Y) *versus* unmodified rAAV2 (mean relative expression: 181 and 779, respectively) (Figure 3A). While these differences were not statistically different owing to the heterogeneity of the data in the rAAV2 group (Figure 3A and S29), the results strongly suggest a benefit of the modified capsid over the unmodified one to allow higher expression levels of the transgene product, as also suggested by RNA transcript levels (Figure S30). Finally, immunohistochemistry analysis showed a significantly higher percentage of GFP-positive cells in the livers of mice injected with rAAV2-GalNAc(Y) *versus* unmodified rAAV2 (mean: 16% and 5%, respectively; p=0.026) (Figure 3B). GFP-positive hepatocytes (in red) were observed in the liver parenchyma of animals injected with rAAV2, mainly distributed as clusters close to portal tracts, with sparse GFP-positive cells detected around centro-lobular veins. By contrast, mice injected with rAAV2-GalNAC(Y) showed a broader distribution of GFP-positive cells, which were clustered around portal tracts and also detected throughout the liver parenchyma and in greater numbers around the portal vein (Figure 3C). Efficient targeting of hepatocytes is the main challenge associated with liver-directed gene therapy, and these data suggest a clear benefit of the Y modified capsid, as evidenced by broader transduction of hepatocytes in mouse liver, despite lower global vector copy numbers than those obtained with the unmodified rAAV2 in the liver tissue. Finally, we assessed levels of eGFP mRNA transcript in non-targeted tissues (*i.e*. heart, skeletal muscle [quadriceps], lung, spleen, and kidney). In all cases, we detected very limited levels of GFP transcript whatever the injected vector. With the rAAV2-GalNAc(Y) vector, eGFP transcripts were observed only in the heart, but at levels approximately 220 times lower than those observed in the liver of the same animals (Table S31). These data show that, at the dose tested, Y-modification of AAV2 does not increase the transduction of non-targeted tissues. Taken together, these findings indicate a positive impact of chemical Y modification of rAAV vectors for hepatocyte targeting *in vivo*. Increasing the number of transduced cells while decreasing vector copy number in these cells are both essential to overcome the efficacy and safety issues that limit the use of AAV vectors for hepatic application.

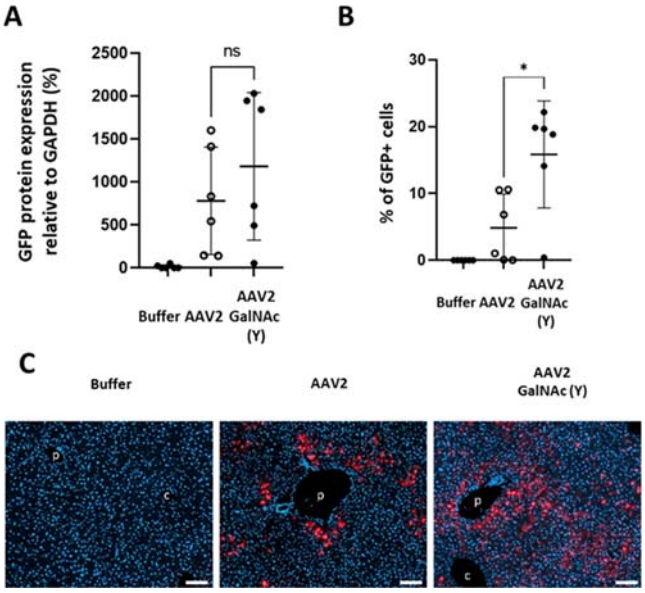

Figure 3: A) Levels of GFP protein expression in mouse liver detected by Western blot 1 month after injection. B) Percentage of GFP-positive cells in liver, detected by GFP immunolabelling. C) Representative image of liver after GFP immunolabelling (red). p, portal vein branches; c, centro-lobular veins. DAPI counter-staining of nuclei is shown in blue. Scale bars=200 µm.

The aim of this project was to develop vectors that can be modified according to the desired target. Therefore, we also used a mannose-derived ligand to generate AAV2-Man(Y), and tested these vectors in retinal tissue, for which multiple gene therapy applications have been developed[30–32]. Prior to *in vivo* injection in the retina, infectivity of AAV2-Man(Y) was evaluated by measuring the ratio of vector genomes (vg) to GFP-forming units (vg/GFU) in HEK293 cells. This ratio is classically used as a quality control measure to evaluate the *in vitro* infectivity of AAV vectors (the higher the ratio the lower the infectivity of the vector). The results showed that rAAV2-Man(Y) vector efficiently transduced HEK293 cells, and as observed for rAAV2-GalNAc(Y), rAAV2-Man(Y) was less infectious in the HEK293 cell line (Table S32).

Retinal transduction efficiency of the modified capsid was next tested *in vivo* in adult wild-type C57/BL6 mice after subretinal injection of unmodified AAV2 or AAV2-Man(Y), both carrying the same CAG-eGFP expression cassette, and a control group was injected with buffer (n=9 per group). *In vivo* fundus fluorescence performed one-month post-injection revealed higher intensity and more broadly distributed fluorescence (white dots) in mice injected with the modified capsid (Figure S33). The quantification of the fluorescence using a plugin in ImageJ software demonstrated a significant increase in the number of fluorescent objects and the overall density of fluorescence in the fundus after transduction of the retina with AAV2-Man(Y) *versus* the unmodified AAV2 capsid (Figure 4A). To validate these *in vivo* findings, GFP fluorescence was evaluated in retinal flatmounts using confocal imaging. For this we distinguish between the region surrounding the injection site itself and the periphery or the region furthest from the injection site. The intensity and distribution of GFP fluorescence at the periphery of the injection site was higher in mice injected with AAV2-Man(Y) versus unmodified AAV2 (Figure 4B), suggesting increased diffusion of the former beyond the subretinal bleb induced by the injection. These data are in line with our observations in liver sections, whereby mice injected with AAV2-GalNAC(Y) showed a broader distribution of GFP-positive cells. Furthermore, while GFP fluorescence around the injection site was comparable in AAV2- and AAV2-Man(Y)-transduced retinas at the level of outer segment (OS), outer nuclear layer (ONL), and inner nuclear layer (INL) (Figure S34), increased fluorescence intensity was observed in the ganglion cell layer (GCL) in all retinas injected with AAV2-Man(Y) (Figure 4C). This suggests either greater AAV2-Man(Y) uptake specifically in ganglion cells or better penetration of the vector through the tissue layers as a consequence of the mannose modification. This increased transduction efficiency in the GCL suggests that these mannose-modified vectors could be coupled with ganglion cell-specific promoters for gene therapy strategies targeting glaucoma or optic neuropathies[33,34]

Taken together, these data show that the AAV2-Man(Y) capsid results in stronger and more widespread retinal transduction than the unmodified AAV2 capsid.

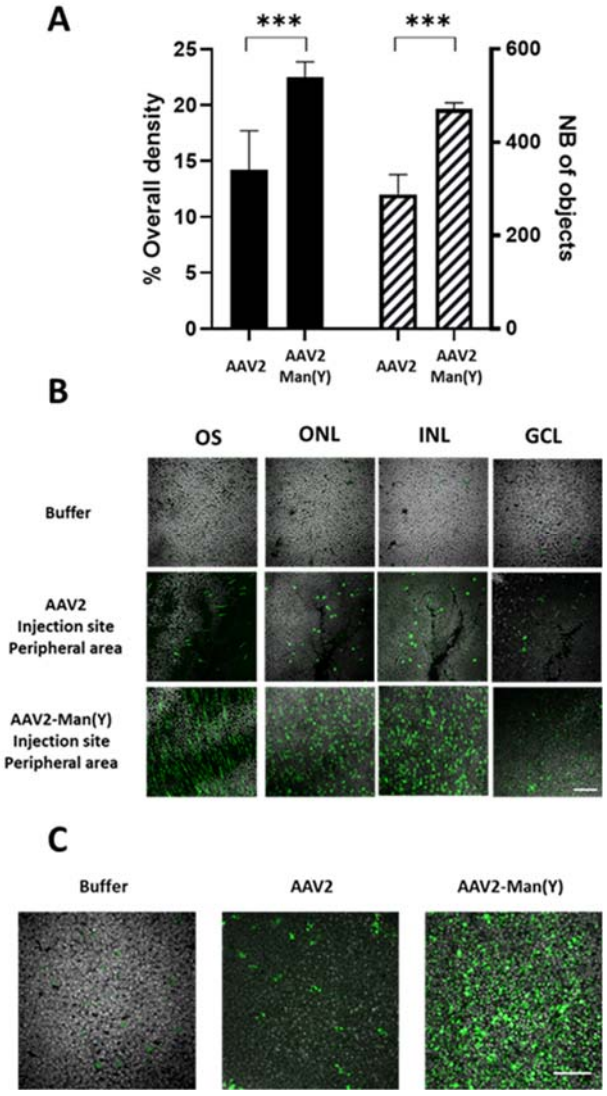

Figure 4: GFP fluorescence study after subretinal injection. A) Quantification of GFP fluorescence in fundus images. Graphs depict the overall density of fluorescence (solid black bars) and number of fluorescent objects (hatched black bars). Both variables were significantly higher (p=0.0002 and p=0.0008 respectively) in mice injected with AAV2-Man(Y) versus unmodified AAV2. B) Representative confocal images of retinal flatmounts of mice injected with either buffer, AAV2 or AAV2-Man(Y) at the periphery of the injection site. Nuclei are stained in grey and GFP fluorescence is displayed in green (scale bar, 10 µm). OS: outer segments, ONL: outer nuclear layer, INL: inner nuclear layer, GCL: ganglion cell layer. C) Representative images of the ganglion cell layer at injection site of retinas injected with buffer, AAV2, or AAV2-Man(Y) are shown. Nuclei are stained in grey and GFP fluorescence is displayed in green (scale bar, 10 µm).

Conclusion

Improvement of vector transduction efficiency is essential to overcome the many challenges implicit in AAV gene therapy. Bioconjugation on the capsid itself may improve targeting, the efficiency of cell entry, and expression of the desired protein. By combining chemistry and vectorology, we have shown that specific ligands can be efficiently grafted onto Y residues of the native AAV2 capsid. To the best our knowledge, this has never been done before.

Using our newly developed chemical capsid engineering platform we observed, both *in vitro* and *in vivo* in the liver and retina, a significant impact on vector transduction efficiency and expression of the gene of interest. In both targets, an increase in the area of transduction and the number of transduced cells was observed for tyrosine-modified versus unmodified rAAVs. Chemical remodeling of therapeutic viruses with diazonium salt may therefore constitute a valuable alternative to genetic engineering methods to improve organ tropism and protein expression in cells. In future studies, this technology will be evaluated with therapeutic transgenes for applications in the liver and retina and extended to other serotypes.

Acknowledgements

The authors thank all personnel at the Boisbonne Center for Gene Therapy (ONIRIS, INSERM, Nantes, France) for handling and care of the rodents used in this study. We also thank the vector core of TaRGeT, UMR 1089 (CPV, INSERM and Nantes Université, which is a bioproduction and biotherapy national integrator (ANR-22-AIBB-0001), http://umr1089.univ-nantes.fr) for the production of the rAAV vectors used in this study. This research was supported by the Fondation d'Entreprise Thérapie Génique en Pays de Loire, the Centre Hospitalier Universitaire (CHU) of Nantes, the Institut National de la Santé et de la Recherche Médicale (INSERM), Nantes Université, and by grants from the French National Agency for Research ("Investissements d'Avenir" Equipex ArronaxPlus.n°ANR-11-EQPX-0004 and ChemAAV (ANR-19-CE18-0001)).

Keywords: Bioconjugation • AAV • Tyrosine • Chemistry • Gene therapy.

[1] H. Zhang, Q. Zhan, B. Huang, Y. Wang, X. Wang, *Front. Cardiovasc. Med.* **2022**, *9*.
[2] J. M. Crudele, J. S. Chamberlain, *Hum. Mol. Genet.* **2019**, *28*, R102–R107.
[3] N. J. Queen, X. Zou, J. M. Anderson, W. Huang, B. Appana, S. Komatineni, R. Wevrick, L. Cao, *Mol. Ther. - Methods Clin. Dev.* **2022**, *27*, 131–148.
[4] E. Lunev, A. Karan, T. Egorova, M. Bardina, *Biomedicines* **2022**, *10*, 1140.
[5] D. W. Russell, M. A. Kay, *Blood* **1999**, *94*, 864–874.
[6] G. Le Meur, P. Lebranchu, F. Billaud, O. Adjali, S. Schmitt, S. Bézieau, Y. Péréon, R. Valabregue, C. Ivan, C. Darmon, P. Moullier, F. Rolling, M. Weber, *Mol. Ther. J. Am. Soc. Gene Ther.* **2018**, *26*, 256–268.
[7] W. Zhan, M. Muhuri, P. W. L. Tai, G. Gao, *Front. Immunol.* **2021**, *12*.
[8] U. T. Hacker, M. Bentler, D. Kaniowska, M. Morgan, H. Büning, *Cancers* **2020**, *12*, 1889.
[9] J. Bennett, A. M. Maguire, *Cold Spring Harb. Perspect. Med.* **2022**, a041307.
[10] H. A. Blair, *CNS Drugs* **2022**, *36*, 995–1005.
[11] L. DeFrancesco, *Nat. Biotechnol.* **2022**, *40*, 1539–1541.
[12] B. A. Hamilton, J. F. Wright, *Front. Immunol.* **2021**, *12*, 675897.
[13] T. Weber, *Front. Immunol.* **2021**, *12*, 658399.
[14] C. Li, R. J. Samulski, *Nat. Rev. Genet.* **2020**, *21*, 255–272.
[15] J. Z. Drago, S. Modi, S. Chandarlapaty, *Nat. Rev. Clin. Oncol.* **2021**, *18*, 327–344.
[16] M. Mével, M. Bouzelha, A. Leray, S. Pacouret, M. Guilbaud, M. Penaud-Budloo, D. Alvarez-Dorta, L. Dubreil, S. G. Gouin, J. P. Combal, M. Hommel, G. Gonzalez-Aseguinolaza, V. Blouin, P. Moullier, O. Adjali, D. Deniaud, E. Ayuso, *Chem. Sci.* **2019**, *11*, 1122–1131.
[17] D. Alvarez Dorta, D. Deniaud, M. Mével, S. G. Gouin, *Chem. Eur. J.* **2020**, *26*, 14257–14269.
[18] S. Depienne, D. Alvarez-Dorta, M. Croyal, R. C. T. Temgoua, C. Charlier, D. Deniaud, M. Mével, M. Boujtita, S. G. Gouin, *Chem. Sci.* **2021**, *12*, 15374–15381.
[19] Q.-Y. Hu, M. Allan, R. Adamo, D. Quinn, H. Zhai, G. Wu, K. Clark, J. Zhou, S. Ortiz, B. Wang, E. Danieli, S. Crotti, M. Tontini, G. Brogioni, F. Berti, *Chem. Sci.* **2013**, *4*, 3827–3832.
[20] E. J. Choi, D. Jung, J.-S. Kim, Y. Lee, B. M. Kim, *Chem. – Eur. J.* **2018**, *24*, 10948–10952.
[21] H. Büning, A. Srivastava, *Mol. Ther. - Methods Clin. Dev.* **2019**, *12*, 248–265.
[22] R. Nakahama, A. Saito, S. Nobe, K. Togashi, I. K. Suzuki, A. Uematsu, K. Emoto, *Mol. Brain* **2022**, *15*, 70.
[23] L. Zhong, B. Li, C. S. Mah, L. Govindasamy, M. Agbandje-McKenna, M. Cooper, R. W. Herzog, I. Zolotukhin, K. H. Warrington, K. A. Weigel-Van Aken, J. A. Hobbs, S. Zolotukhin, N. Muzyczka, A. Srivastava, *Proc. Natl. Acad. Sci.* **2008**, *105*, 7827–7832.
[24] L. Zhong, B. Li, G. Jayandharan, C. S. Mah, L. Govindasamy, M. Agbandje-McKenna, R. W. Herzog, K. A. Weigel-Van Aken, J. A. Hobbs, S. Zolotukhin, N. Muzyczka, A. Srivastava, *Virology* **2008**, *381*, 194–202.
[25] O. Pieroni, A. Fissi, J. L. Houben, *Makromol. Chem.* **1975**, *176*, 3201–3209.
[26] O. Khorev, D. Stokmaier, O. Schwardt, B. Cutting, B. Ernst, *Bioorg Med Chem* **2008**, *16*, 5216–31.
[27] M. Mével, V. Pichard, M. Bouzelha, D. Alvarez-Dorta, P.-A. Lalys, N. Provost, M. Allais, A. Mendes, E. Landagaray, J.-B. Ducloyer, A. Galy, N. Brument, G. M. Lefevre, S. G. Gouin, C. Isiegas, G. L. Meur, T. Cronin, C. L. Guiner, M. Weber, P. Moullier, E. Ayuso, D. Deniaud, O. Adjali, **2022**, 2022.12.01.518481.
[28] M. Tanowitz, L. Hettrick, A. Revenko, G. A. Kinberger, T. P. Prakash, P. P. Seth, *Nucleic Acids Res.* **2017**, *45*, 12388–12400.
[29] J. O'Donnell, K. A. Taylor, M. S. Chapman, *Virology* **2009**, *385*, 434–443.
[30] J.-B. Ducloyer, G. Le Meur, T. Cronin, O. Adjali, M. Weber, *Med. Sci. MS* **2020**, *36*, 607–615.
[31] M. Pavlou, C. Schön, L. M. Occelli, A. Rossi, N. Meumann, R. F. Boyd, J. T. Bartoe, J. Siedlecki, M. J. Gerhardt, S. Babutzka, J. Bogedein, J. E. Wagner, S. G. Priglinger, M. Biel, S. M. Petersen-Jones, H. Büning, S. Michalakis, *EMBO Mol. Med.* **2021**, *13*, e13392.
[32] I. Trapani, P. Tornabene, A. Auricchio, *Gene Ther.* **2021**, *28*, 220–222.
[33] K. S. Hanlon, N. Chadderton, A. Palfi, A. Blanco Fernandez, P. Humphries, P. F. Kenna, S. Millington-Ward, G. J. Farrar, *Front. Neurosci.* **2017**, *11*.
[34] B. Nieuwenhuis, E. Laperrousaz, J. R. Tribble, J. Verhaagen, J. W. Fawcett, K. R. Martin, P. A. Williams, A. Osborne, *Gene Ther.* **2023**, DOI 10.1038/s41434-022-00380-z.

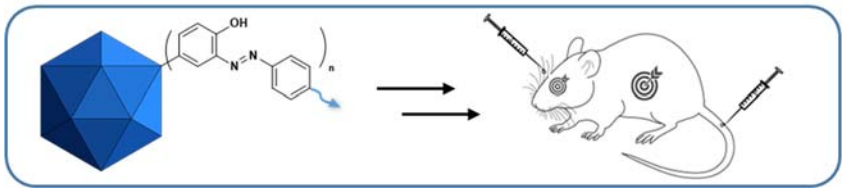

To increase the transduction efficiency of adeno-associated virus-based vectors, we developed a bioconjugation strategy to chemically modify the tyrosine on the capsid surface. We demonstrated the feasibility of this AAV vector modification strategy using a specific ligand, which increased transduction in both the liver and retina *in vivo*.